THE JOURNAL OF BIOLOGICAL CHEMISTRY VOL. 284, NO. 18, pp. 12504–12511, May 1, 2009

Identification of the Small Protein Rich in Arginine and Glycine (SRAG)

A NEWLY IDENTIFIED NUCLEOLAR PROTEIN THAT CAN REGULATE CELL PROLIFERATION[*S]

Received for publication, December 16, 2008, and in revised form, February 27, 2009 Published, JBC Papers in Press, March 2, 2009, DOI 10.1074/jbc.M809436200

Alfred J. Zullo[‡], Monia Michaud[‡], Weiping Zhang[§], and Michael J. Grusby[‡1]

From the [‡]Department of Immunology and Infectious Disease, Harvard School of Public Health, Boston, Massachusetts 02115 and the [§]Department of Pathophysiology, Second Military Medical University, Shanghai 200433, China

The characterization of new proteins will aid in our explanation of normal biology and disease. Toward that goal, we describe the initial characterization of the small protein rich in arginine and glycine (SRAG). Human and mouse SRAG are 248/249-amino acid arginine- and glycine-rich proteins that are widely expressed in tissues and cell lines. Two SRAG isoforms, SRAG-5 and SRAG-3, which are truncations of full-length SRAG, were also identified. Although all SRAG proteins reside in the nucleus, they were also found within the nucleolus. Localization within the nucleolus was regulated by the N terminus of the protein. Our initial studies indicated that SRAG can interact with RNA. Full-length SRAG protein levels were highest in resting cells and were reduced in proliferating cells. The reduction in SRAG protein that occurs in proliferating cells was mapped with inhibitors to the G_2/M phase of the cell cycle. As expected, the overexpression of SRAG reduced the percentage of cells in the G_2/M phase and increased cell death. In sum, we have identified a new and intriguing member of the nucleolar proteome.

The combination of genome sequencing and mass spectrometry screening has revealed a myriad of uncharacterized proteins, the study of which will enhance our understanding of normal biology and disease. In the course of performing yeast-two-hybrid screens for signal transducer and activator of transcription (STAT)[2]-interacting proteins (1), we identified a 248-amino acid protein that lacks known protein domains and is rich in arginine and glycine. This protein has been named small protein rich in arginine and glycine (SRAG) and is identical to the predicted protein product of the human C1orf77 gene. To date, a small amount of information regarding SRAG has been deposited in public databases. In the course of characterizing proteins encoded in the human major histocompatibility complex class III region, yeast-two hybrid analysis detected an interaction between SRAG and a member of the DEAD box family of RNA helicases known as BAT1 (2). Mass spectrometry analysis of global phosphorylation networks suggests that SRAG is phosphorylated at the C terminus (3). Finally large scale cDNA transfection experiments have implicated a role for SRAG in cell growth (4).

In the current work, we describe the cloning of three SRAG proteins. In addition to a full-length SRAG (FL-SRAG), two additional isoforms, SRAG-5 and SRAG-3, were also isolated. We localized SRAG proteins to both the nucleus and nucleolus of cells. We determined that the N terminus of FL-SRAG acts to exclude SRAG from the nucleolus. Consistent with its localization within the RNA-rich nucleolus, we determined that SRAG can interact with RNA. Lastly we determined that SRAG protein levels are reduced in proliferating cells at the G_2/M stage of the cell cycle. Overexpression of SRAG can reduce passage through G_2/M and enhance cell death. In sum, we have identified a new and complex member of the evolving nucleolar proteome.

EXPERIMENTAL PROCEDURES

Cloning of SRAG—Total RNA was isolated from HeLa cells by TRIzol (Invitrogen) extraction, and cDNA was prepared with the iScript cDNA synthesis kit (Bio-Rad). Human SRAG (C1orf77 mRNA) was amplified from HeLa cell cDNA using the following primers that are based upon GenBank™/NCBI accession number BC120962: C1orf77 For, 5′-ATGGCTGCACAGTCA-3′; C1orf77 Rev, 5′ TCAATCATTGGTTTCGGGATC-3′. PCR amplification was performed with *Taq* Platinum, which permitted the cloning of PCR products into the pTARGET vector (Promega). Standard cloning methods were use to produce GFP fusion constructs in the pEGFP-N1 vector (Clontech).

Protein Alignment—Amino acid sequences for human nucleolin (NP_005372), fibrillarin (NP_001427), and SRAG/C1orf77 (NP_056422) were obtained from NCBI. The alignment of human SRAG, nucleolin, and fibrillarin was performed using Geneious Basic v3.85 using a Blosum62 matrix. The multiple organism alignment was prepared similarly using the following additional sequences: mouse SRAG (BAE31263), *Xenopus* SRAG (NP_001011271), zebrafish SRAG (NP_955840), and chicken SRAG (XP_424013).

Anti-SRAG Antiserum—Rabbit anti-SRAG antiserum was generated by immunization with amino acids 235–248 derived

* The work was supported by a gift from the G. Harold and L. Mathers Charitable Foundation (to M. J. G.) and an Arthritis Foundation postdoctoral fellowship (to A. J. Z.).

[S] The on-line version of this article (available at http://www.jbc.org) contains supplemental Figs. 1 and 2.

[1] To whom correspondence should be addressed: Dept. of Immunology and Infectious Disease, Harvard School of Public Health, FXB Rm. 205, 651 Huntington Ave., Boston, MA 02115. Tel.: 617-432-1240; Fax: 617-432-0084; E-mail: mgrusby@hsph.harvard.edu.

[2] The abbreviations used are: STAT, signal transducer and activator of transcription; SRAG, small protein rich in arginine and glycine; FL-SRAG, full-length SRAG; HSP, heat shock protein; UBF, upstream binding factor; Th1, T helper type I; Th2, T helper type II; GFP, green fluorescent protein; eGFP, enhanced green fluorescent protein; PBS, phosphate-buffered saline; shRNA, short hairpin RNA; Pipes, 1,4-piperazinediethanesulfonic acid.

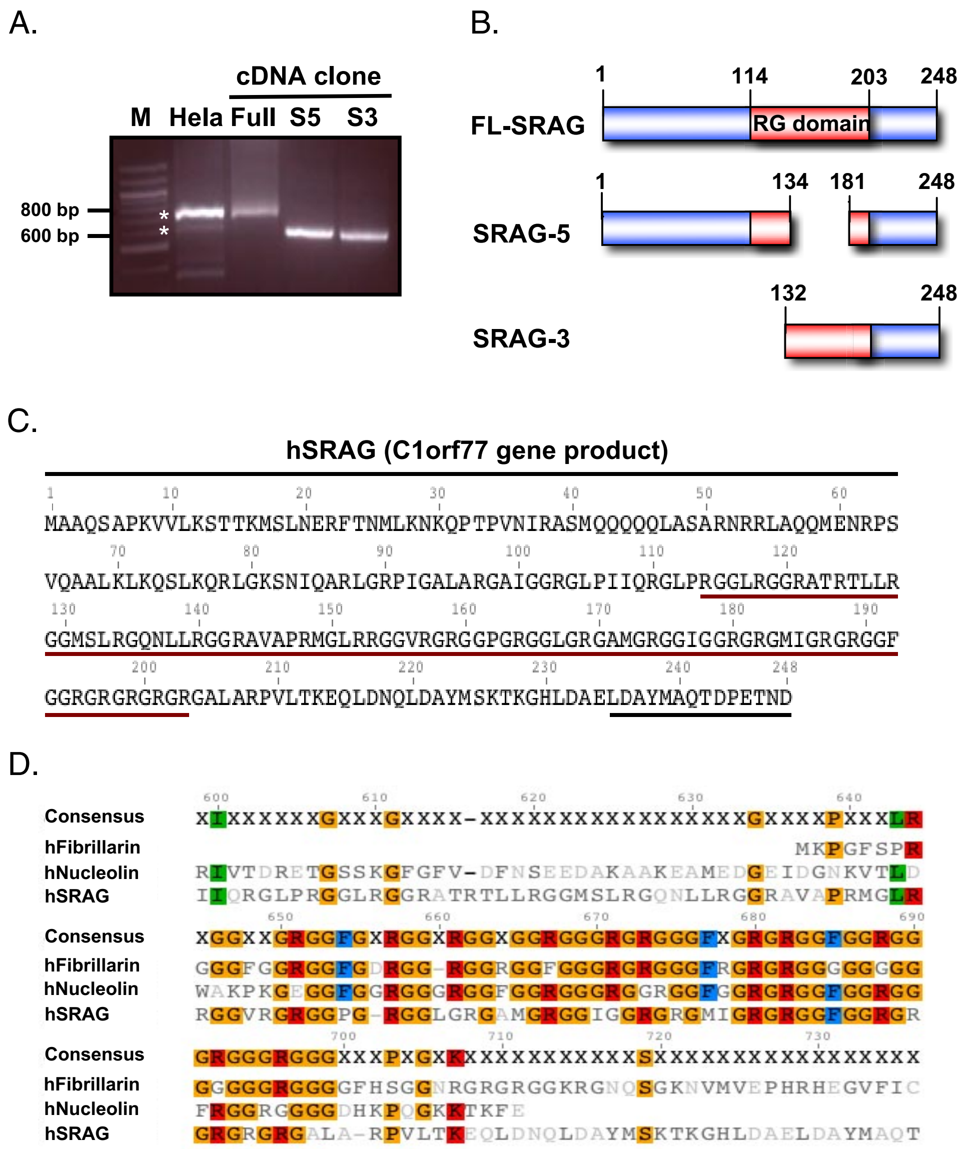

FIGURE 1. **Cloning and identification of SRAG.** *A*, reverse transcription-PCR of human SRAG from HeLa cells. HeLa cell cDNA was amplified with primers at the ATG and TGA of human SRAG/C1orf77 cDNA. *Asterisks* identify the full-length cDNA and the cDNA giving rise to isoforms SRAG-5 (*S5*) and SRAG-3 (*S3*). As reference controls, PCR products from cloned FL-SRAG, SRAG-5, and SRAG-3 are included. Shown are PCR results from at least two experiments with the indicated primers. *M*, molecular size markers. *B*, schematic of SRAG proteins cloned in this study. *C*, amino acid sequence of human SRAG (*hSRAG*). A *black line* denotes the peptide used to generate anti-SRAG antiserum. A *red line* identifies the arginine/glycine-rich region. *D*, amino acid alignment of the arginine/glycine-rich regions of human (*h*) nucleolin, fibrillarin, and SRAG.

from human SRAG (Sigma-Genosys). The antiserum obtained from the final bleed was used for all experiments.

Mouse Tissue Lysates—C57BL/6 or Balb/c mice were euthanized by CO_2 asphyxiation, and tissues were homogenized in 1× radioimmune precipitation assay buffer supplemented with protease inhibitors. After sitting on ice for 30 min with frequent vortexing, the lysates were cleared by centrifugation, and protein was quantified by BCA assay (Pierce).

Cell Culture—HeLa and 293T cells were maintained in Dulbecco's modified Eagle's medium supplemented with 10% fetal bovine serum, L-glutamine, non-essential amino acids, sodium pyruvate, penicillin/streptomycin, and 2-mercaptoethanol. All experiments were conducted at 37 °C and 5% CO_2. 2D6 cells were cultured as described previously (5).

Western Blotting—Cell fractions or total cell extracts were quantified by BCA assay and resolved by SDS-PAGE. Proteins were transferred to polyvinylidene difluoride, and membranes were blocked in 5% nonfat dry milk in Tris-buffered saline. Membranes were probed with the following antibodies in nonfat dry milk/Tris-buffered saline: anti-SRAG antiserum (1:2000), anti-heat shock protein (HSP) (1:1000; Santa Cruz Biotechnology), anti-upstream binding factor (UBF) (1:1000; Santa Cruz Biotechnology), and anti-proliferating cell nuclear antigen (1:1000; Santa Cruz Biotechnology). After washing and probing with the appropriate secondary antibodies (Zymed Laboratories Inc.), proteins were revealed by chemiluminescence (Pierce).

Nuclear Extraction—Total nuclear extracts were prepared using the NE-PER kit (Pierce) according to the manufacturer's instructions.

Isolation of Nucleoli from Primary Lymphocytes—Lymphocyte nucleoli were isolated using a modification of the Lamond laboratory protocol.[3] Briefly ~7.0 × 10^7 lymphocytes were cultured for 2 days under neutral, Th1, or Th2 conditions as described in Tanaka and coworkers (1, 5). Cells were washed in PBS, resuspended in 1.25 ml of buffer A (10 mM Hepes pH 7.9, 10 mM KCl, 1.5 mM $MgCl_2$, 0.5 M DTT), and allowed to swell for 10 min on ice. 15 μl of 10% Nonidet P-40 was added, and the tubes were rocked gently. 3 ml of buffer S1 (0.25 M sucrose, 10 mM $MgCl_2$) was added, and the mixture was briefly sonicated. The mixture was layered over 4 ml of buffer S2 and centrifuged at 1430 × *g* for 5 min. The resulting nuclei were resuspended in buffer S2 (0.35 M sucrose, 0.5 mM $MgCl_2$) and sonicated vigorously to release nucleoli. The process was monitored by phase-contrast microscopy. The resulting nucleoli mixture was layered over 3 ml of buffer S3 (0.88 M sucrose, 0.5 mM $MgCl_2$) and centrifuged at 3000 × *g*. The nucleolar pellet was washed in 500 μl of buffer S2, centrifuged at 1430 × *g*, and transferred in 100 μl of buffer S2 into an Eppendorf tube. Proteins were extracted with the addition of 5× radioimmune precipitation assay buffer and vigorous vortexing.

[3] A. Lamond, personal communication.

Transfection—HeLa cells were split the day of transfection and were allowed to adhere for 1–2 h prior to transfection. HeLa cells were transfected with 300–600 ng of plasmid DNA with Effectene (Qiagen) according to the manufacturer's instructions. For the transfection of shRNAs, control and anti-C1orf77 (SRAG) shRNAs were purchased from Invitrogen. HeLa and 293T cells were transfected with Lipofectamine RNAiMAX according to the manufacturer's instructions (Invitrogen). After 18 h, the cells were harvested, and Western blots were performed.

Immunofluorescence Microscopy—HeLa cells were transfected on 18-mm glass coverslips for 18–24 h. The coverslips were washed in PBS and fixed with 4% formalin, PBS for 10 min. For the imaging of tagged proteins, the coverslips were then stained with Hoescht and mounted in Aqua Polymount. For UBF staining, the fixed cells were permeabilized in 0.1% Triton, PBS; blocked in 5% fetal bovine serum, PBS; and stained for 1.5 h at room temperature at a 1:200 dilution. After washing in 0.1% Triton, PBS, the coverslips were stained with goat anti-mouse 647 for 45 min at room temperature. After washing, the coverslips were stained with Hoescht and mounted in Aqua Polymount. All images were taken on an Olympus IX81 confocal microscope at 100× magnification.

Native Gel Electrophoresis—293T cells were transfected with FL-SRAG, and nuclear extracts were prepared. 15 μg of each extract was incubated in 15 mM Hepes, 100 mM KCl, 0.2 mM EDTA, 5 mM $MgCL_2$, 10% glycerol, 1 mM dithiothreitol, 0.05% Nonidet P-40, 0.4 μg/ml bovine serum albumin for 15 min on ice. RNase or DNase was added, and the extracts were incubated on ice for 15 min and at room temperature for 15 min and then resolved by native 4% PAGE at pH 8.3 with Tris borate-EDTA as the buffer. The gel was then transferred to polyvinylidene difluoride, and Western blotting for SRAG was performed as described above.

RNase/DNase Treatment of Transfected Coverslips—Assays were performed similarly to that described previously (6). HeLa cells were transfected with FL-SRAG as described above. Coverslips were washed in PBS and CSK buffer (10 mM Pipes, 100 mM NaCl, 300 mM sucrose, 3 mM $MgCl_2$). Cells were permeabilized/extracted in CSK buffer + 0.1% Triton X-100. After washing with CSK buffer and PBS, coverslips were treated for 9 min with either RNase A (1 mg/ml in PBS) or DNase (1 unit/μl) in matched buffer). After washing, coverslips were fixed with 2% formalin, PBS; stained with Hoescht; and mounted in Aqua Polymount.

Cell Cycle Analysis by Propidium Iodide Staining—Staining for cell cycle analysis was performed essentially as described previously (7). Briefly cells were trypsinized and resuspended in 1 ml of PBS. 1 ml of 80% ethanol was added, the tubes were vortexed, and the cells were fixed at 4 °C for 30 min. After centrifuging at 863 × g for 5 min, the cells were treated with 50 μg/ml RNase A for 45 min at 37 °C. After washing with PBS, the cells were resuspended in 46 ng/ml propidium iodide in sodium citrate. Cells were stained for 30 min and analyzed on a BD LSRII flow cytometer. In each case, transfected cells were identified as GFP^+ cells, which were then analyzed for propidium iodide.

Cell Death Measured by Propidium Iodide Uptake—Transfected HeLa cells were treated essentially as described previously (7). Briefly medium and trypsinized cells were combined and centrifuged at 863 × g for 5 min. The cells were washed with PBS and resuspended in 250 μl of PBS. After vortexing, 360 μl of propidium iodide solution was added, the cells were allowed to sit for 5 min at room temperature, and propidium iodide uptake among GFP^+ cells was assayed by flow cytometry.

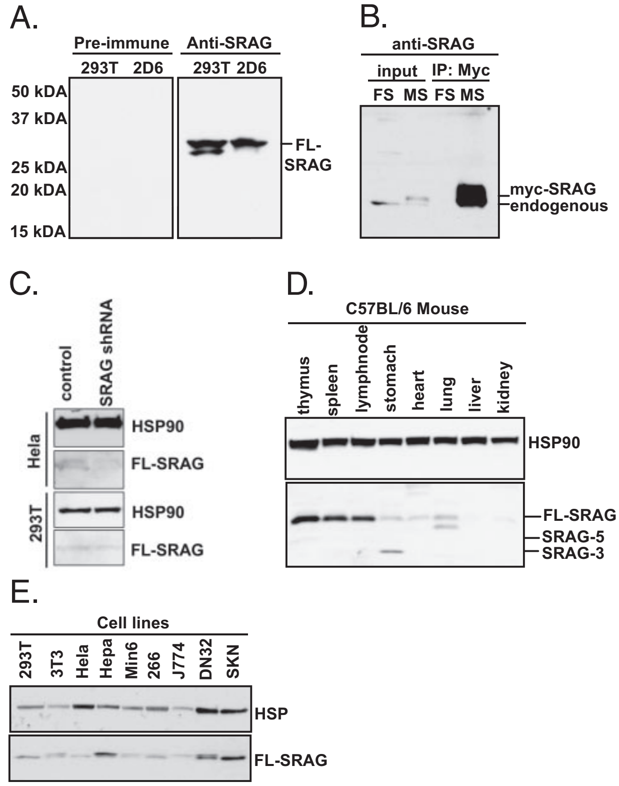

FIGURE 2. **Expression of SRAG.** *A*, Western blot of 293T and 2D6 total protein extracts with either preimmune serum or anti-SRAG antiserum. FL-SRAG, which is the only SRAG protein detected in cell lines, is shown. Shown are data from two similar experiments. *B*, 293T cells were transfected with a Myc-SRAG (*MS*) construct or a control construct containing a frameshift (*FS*) mutation. Immunoprecipitation (*IP*) against the Myc epitope was performed. Total lysates and the immunoprecipitates were resolved by SDS-PAGE, and a Western blot with anti-SRAG antiserum was performed. The Myc-SRAG contains a linker between the epitope tag and SRAG thus making the transfected SRAG a little larger than endogenous SRAG. Shown are data from two similar experiments. *C*, HeLa and 293T cells were transfected with either control shRNA or anti-SRAG shRNA. After 18 h, the cells were harvested, and a Western blot with anti-HSP90 and anti-SRAG antiserum was performed. *D*, Western blot analysis of mouse tissues with anti-SRAG antiserum. FL-SRAG, SRAG-5, and SRAG-3, which are expressed at different levels in specific tissues, are identified. Shown are data representative of two experiments. *E*, Western blot of common laboratory cell lines for control HSP90 and SRAG.

RESULTS

SRAG Is the Human C1orf77 Protein Product—SRAG was identified in a yeast two-hybrid screen designed to identify STAT-interacting proteins (1). Although a functional role for SRAG in STAT biology remains unclear, we decided to clone the cDNA from human cells and characterize the basic biology of the protein. Sequence obtained from the yeast two-hybrid clone suggested that SRAG would be the protein product of human C1orf77. To confirm that SRAG/C1orf77 was expressed in mammalian cells, primers at the beginning and end of the C1orf77 gene product were used to amplify cDNA prepared

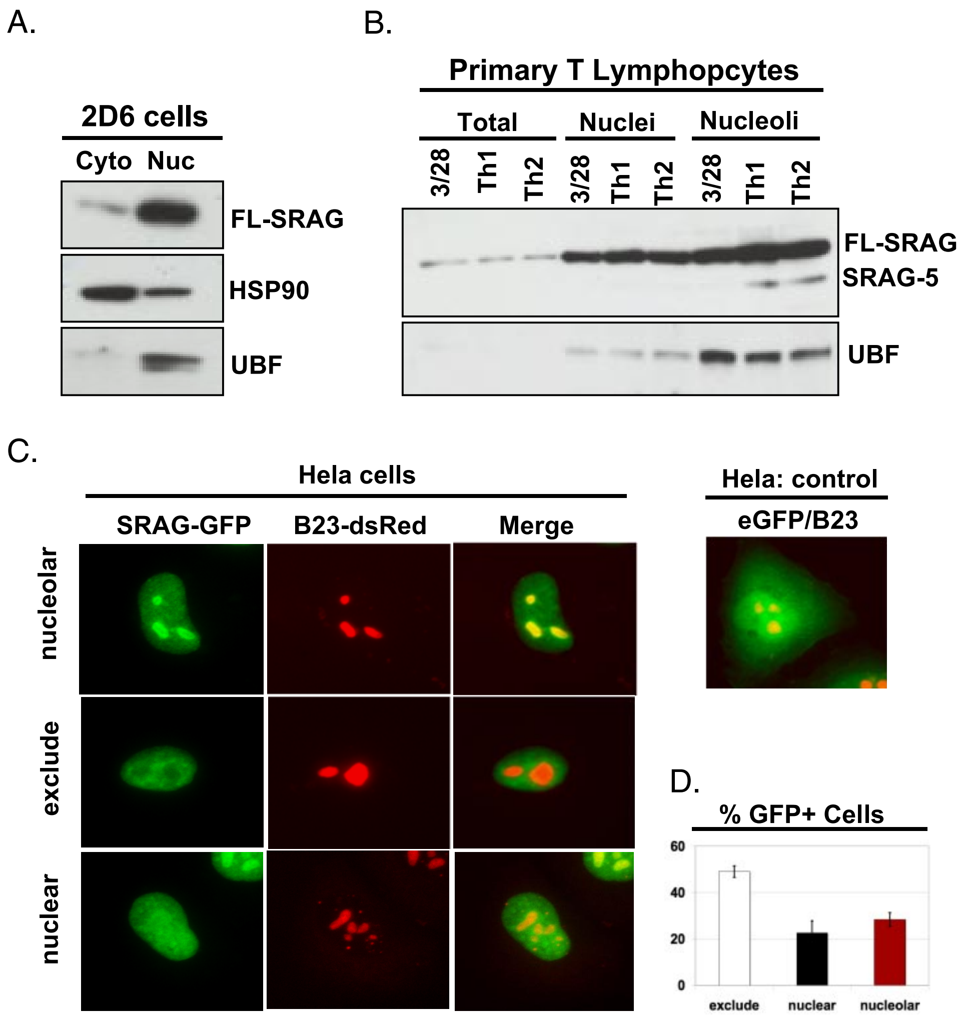

FIGURE 3. **SRAG is found in the nucleus and nucleolus.** *A*, Western blot of nuclear (*Nuc*) and cytosolic (*Cyto*) extracts from 2D6 cells with anti-SRAG, -cytosolic HSP90, and -nucleolar UBF is shown. Shown are data representative of two experiments. *B*, Western blot of total, nuclear, and nucleolar protein lysates from primary lymphocytes with anti-SRAG and anti-UBF. *3/28* refers to cells activated with anti-CD3$^+$ anti-CD28 antibodies. *Th1* and *Th2* refer to cells cultured under T helper type I and type II conditions, respectively. Shown are data representative of two experiments. *C*, confocal microscopy of HeLa cells transfected with 300 ng of FL-SRAG-GFP and 250 ng of B23-dsRed. Shown are the three states in which SRAG was found within HeLa cells. Cells transfected with eGFP and B23-dsRed serve as the comparative control. Shown are data representative of two experiments. *D*, FL-SRAG was transfected into HeLa cells, and the number of cells with nucleolar, nuclear, or excluded SRAG, as defined in *C*, was counted. Shown is the percentage of each population and the S.D. (*error bars*) derived from three experiments. More than 100 cells were evaluated.

from HeLa cells. As shown in Fig. 1*A*, two bands were obtained between 600 and 800 bp (Fig. 1*A*). The bands were cloned by TA cloning and sequenced. The ≅800-bp product was found to encode a 248-amino acid protein that was identical to FL-SRAG cDNA obtained from our yeast two-hybrid screen (Fig. 1, *B* and *C*). The ≅600-bp PCR product was found to encode two additional isoforms, SRAG-5 and SRAG-3, that appear to be derived from alternative splicing of the FL-SRAG cDNA (Fig. 1*B*). Analysis of the FL-SRAG amino acid sequence revealed a lack of known protein domains. As a result, SRAG bears limited homology with other mammalian proteins. SRAG does contain an arginine/glycine-rich region similar to that found in nucleolin and fibrillarin (Fig. 1*D*). In sum, FL-SRAG and SRAG isoforms appear to be protein products of the human C1orf77 gene. Comparison of SRAG amino acid sequences from mammals, zebrafish, and *Xenopus* indicated that SRAG is highly conserved (supplemental Fig. 1). Thus far, a SRAG gene has not been found in other model organisms including yeast, *Caenorhabditis elegans*, and *Drosophila*.

SRAG Antiserum—To further characterize SRAG expression, antiserum was raised against amino acids 235–248 of human SRAG. Because FL-SRAG and isoforms contain this C terminus, SRAG antiserum detects all SRAG proteins identified to date. Both human SRAG and murine SRAG share the same peptide used for immunization allowing us to query both human and mouse cells. Western blot analysis of human 293T and murine 2D6 cells with anti-SRAG antiserum identified FL-SRAG as either a single band or doublet that is ~28 kDa (Fig. 2*A*). In contrast, preimmune serum failed to recognize these proteins. Western blot analysis of overexpressed Myc-SRAG with anti-SRAG antiserum supported the ability of SRAG antiserum to identify FL-SRAG (Fig. 2*B*). Lastly Western blot of HeLa and 293T cells transfected with an shRNA that targets the SRAG mRNA confirmed that our antiserum correctly identified FL-SRAG (Fig. 2*C*).

SRAG Is Broadly Expressed—Analysis of a panel of common laboratory cell lines revealed that FL-SRAG was expressed (Fig. 2*E*). SRAG-5 and SRAG-3 were not detected at significant levels in cell lines. Western blot analysis of mouse tissues confirmed that although FL-SRAG is broadly expressed the highest levels are found in thymus, spleen, and lymph nodes (Fig. 2*D*). In contrast, only trace amounts of SRAG-5 were detected in the thymus, and SRAG-3 has thus far only been identified in the stomach (Fig. 2*D*).

SRAG Is a Nuclear and Nucleolar Protein—SRAG shares little homology to other mammalian proteins. However, like the nucleolar proteins nucleolin and fibrillarin, SRAG contains an arginine/glycine-rich region. This limited similarity suggested that SRAG would be located in the nucleus and the nucleolus. To test for a nuclear localization, 2D6 cells were fractionated into cytosolic and nuclear fractions, and Western blotting for SRAG, cytosolic HSP90, and nucleolar UBF was performed. As shown in Fig. 3*A*, SRAG was found primarily in the nucleus (Fig. 3*A*). To test whether SRAG could be detected in the nucleolus,

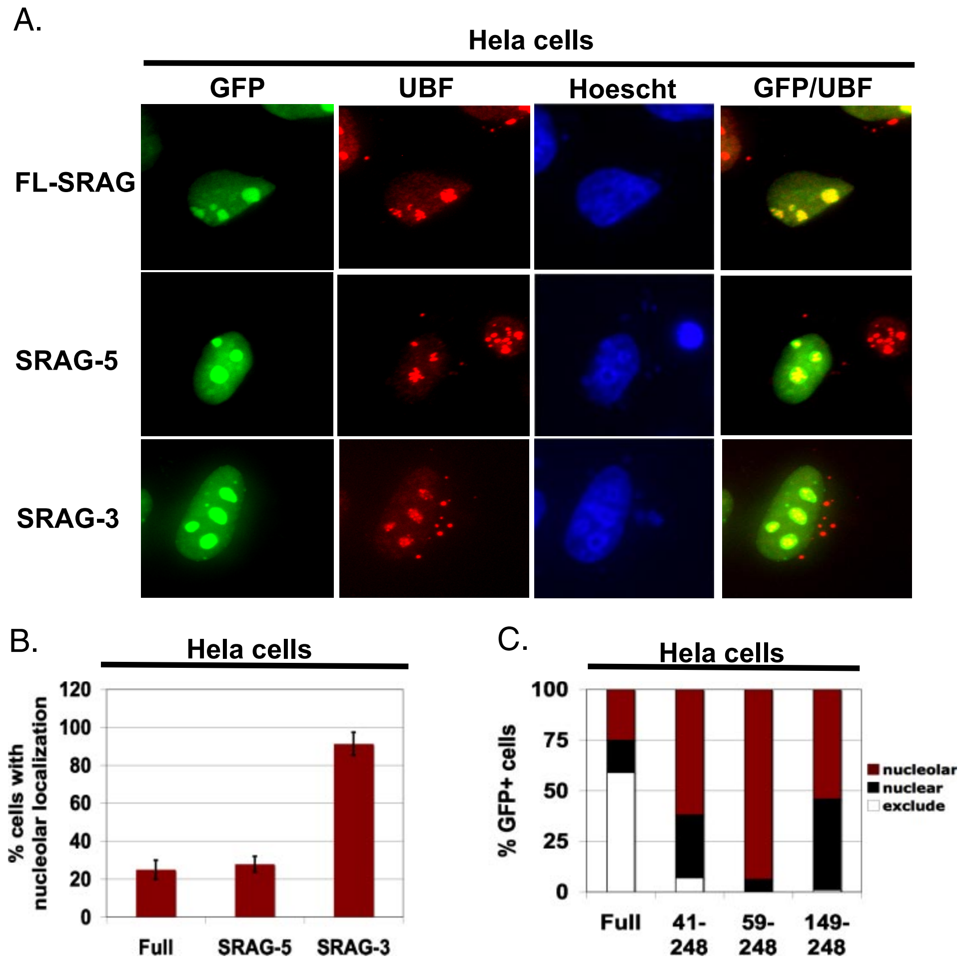

FIGURE 4. **The N terminus of SRAG regulates localization within the nucleolus.** *A*, FL-SRAG-GFP, SRAG-5-GFP, and SRAG-3-GFP were transfected into HeLa cells. After 24 h, the cells were stained for endogenous UBF and counterstained with Hoescht. Results representative of two similar experiments are shown. *B*, HeLa cells were transfected for 24 h with FL-SRAG-GFP, SRAG-5-GFP, and SRAG-3-GFP. The cells were then stained with Hoechst, and the number of cells in which SRAG was found within the nucleolus was quantified; the percentage is given. Shown is the average and S.D. (*error bars*) of one experiment performed in triplicate. At least 100 cells per isoform were evaluated. *C*, HeLa cells were transfected with either FL-SRAG-GFP or engineered GFP-tagged mutants for 24 h. The cells were then stained with Hoescht; the number of cells with nucleolar, excluded, and nuclear SRAG, as described in Fig. 3*C*, was counted; and the percentage was determined. Shown are data representative of two experiments. At least 100 cells per mutant were evaluated.

primary splenocytes were activated with anti-CD3 plus anti-CD28 or skewed under Th1 or Th2 conditions (1, 5). We chose to use activated T lymphocytes as large numbers of this primary cell can be quickly cultured *in vitro*. Total, nuclear, and nucleolar protein extracts were prepared, and a Western blot was performed for SRAG and nucleolar UBF. As shown in Fig. 3*B*, UBF was enriched as the cells were fractionated, and a significant quantity of FL-SRAG and SRAG-5 was identified in the UBF-enriched nucleolar fractions. (Fig. 3*B*). SRAG-3 was not observed in nucleolar protein fractions. To further confirm SRAG localization, FL-SRAG was cloned into pEGFP-N1 to produce an FL-SRAG-GFP fusion protein. FL-SRAG-GFP and B23-dsRed (a generous gift from A. Lamond, University of Dundee, Dundee, Scotland, UK), a well characterized nucleolar protein, were transfected into HeLa cells, and localization was determined by confocal fluorescence microscopy. Although SRAG was always nuclear, ~25–35% of HeLa cells localized SRAG with B23 in the nucleolus (Fig. 3, *C* and *D*). In the remaining cells, SRAG appeared either broadly nuclear or was excluded from the nucleolus (Fig. 3, *C* and *D*). SRAG is therefore both a nuclear and nucleolar protein.

The N Terminus Regulates SRAG Localization within the Nucleolus—Although all SRAG isoforms identified to date can inhabit the nucleolus (Fig. 4*A*), we noticed that they did so with different frequencies. Although FL-SRAG-GFP and SRAG-5-GFP were found in the nucleolus in 25–35% of HeLa cells, SRAG-3-GFP, which is missing 131 N-terminal amino acids, was nucleolar in nearly 100% of HeLa cells (Fig. 4*B*). This suggested that the N terminus of SRAG was responsible for excluding SRAG from the nucleolus. To test this idea further, artificial SRAG mutants were generated as GFP fusion proteins. Removal of as little as 40 N-terminal amino acids increased the number of cells with nucleolar SRAG (Fig. 4*C*). As a result, our data suggest that the N terminus regulates the exclusion of SRAG from the nucleolus.

SRAG Responds to Changes in RNA—In the course of identifying conditions suitable for SRAG extraction and Western blotting, we noticed that extraction with Nonidet P-40 failed to remove all of the SRAG protein from cells. Re-extraction of the Nonidet P-40-insoluble pellet with radioimmune precipitation assay buffer liberated the remaining SRAG protein (Fig. 5*A*). This indicated that a portion of SRAG is tightly bound within the nucleus and suggested an interaction with nucleic acid. To test this, FL-SRAG was transfected into 293T cells, and nuclear extracts were prepared. We took advantage of the fact that SRAG is positively charged and has a predicted pI of greater than 12.0. However, if SRAG was bound to nucleic acid, the charge would be neutralized permitting greater mobility on a native gel at pH 8.3. It was predicted that treatment with RNase or DNase would reduce SRAG mobility in these assays. Nuclear extracts were incubated with either RNase or DNase and then resolved by native PAGE. After transferring to polyvinylidene difluoride, a Western blot to SRAG was performed. SRAG mobility in these assays was reduced by treatment with RNase but not DNase suggesting that SRAG could interact with RNA (Fig. 5*B*). To test this further, HeLa cells growing on coverslips were transfected with FL-SRAG-GFP. After a brief permeabilization to remove loosely bound proteins, the cells were treated with either RNase or DNase. After washing and fixation, the cells were analyzed by microscopy. Treatment of coverslips with DNase had only

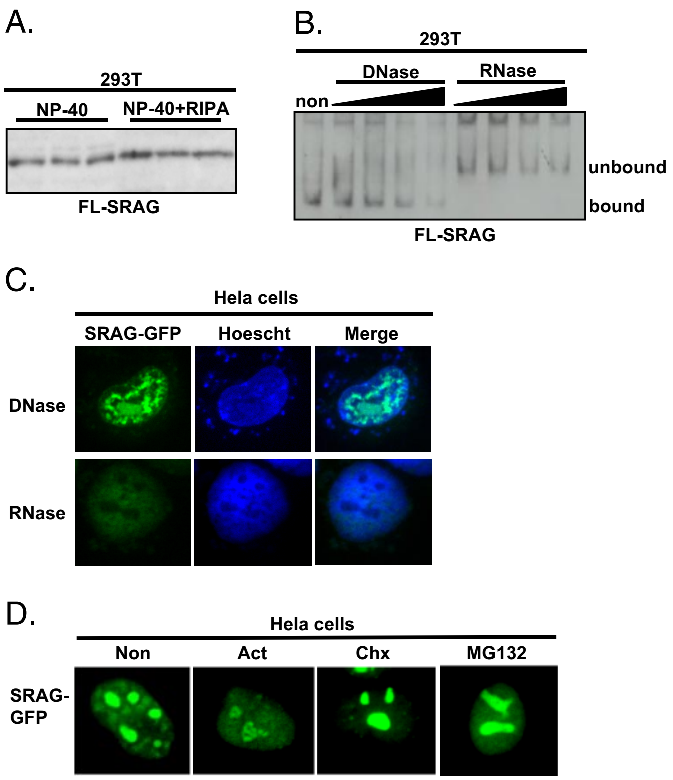

FIGURE 5. **SRAG can interact with RNA.** *A*, 293T cells were first extracted in an Nonidet P-40 (*NP-40*)-based lysis buffer (1). After washing in the same, the insoluble pellet was re-extracted in radioimmune precipitation assay (*RIPA*) buffer. Both fractions were resolved by SDS-PAGE, and a Western blot for SRAG was performed. Shown are data representative of multiple observations. *B*, nuclear extracts from FL-SRAG-transfected 293T cells were treated with DNase or RNase and resolved by native PAGE. Treatment with RNase, but not DNase, removed interacting RNA and thus slowed SRAG migration under these conditions. Shown are data representative of two experiments. *non*, untreated. *C*, HeLa cells were transfected with FL-SRAG on coverslips that were then treated with DNase or RNase. After washing and fixation, the cells were stained with Hoescht and imaged. Shown are data representative of two experiments. *D*, HeLa cells were transfected with FL-SRAG-GFP. After 24 h, the cells were treated with actinomycin D (*Act*; 1 μg/ml), cycloheximide (*Chx*; 50 μg/ml), and MG132 (10 μM) for 75 min. The cells were then fixed, counterstained with Hoescht, and analyzed by microscopy. Shown are data representative of three experiments. *Non*, untreated.

minor effects on SRAG as evidenced by the presence of cells with robust nucleolar staining for SRAG (Fig. 5*C*). In contrast, treatment with RNase removed nucleolar SRAG and reduced the overall fluorescence of the cells (Fig. 5*C*). To further confirm this hypothesis, HeLa cells grown on glass coverslips were transfected with FL-SRAG-GFP and treated with actinomycin D. Actinomycin D is a potent inhibitor of transcription that has been extensively utilized to investigate RNA-binding proteins such as those that compose the nucleolus (8). Nucleolar SRAG had a smooth appearance and completely occupied the nucleolus of cells. However, treatment with actinomycin D for only 75 min reduced the overall fluorescence of nucleolar SRAG and resulted in the formation of SRAG-deficient holes or pits within the nucleolus (Fig. 5*D*). Other inhibitors including MG132 and cycloheximide, which induce nucleolar stress through different mechanisms (8), did not affect the nucleolar appearance of SRAG (Fig. 5*D*). Similarly treatment with aphidicolin, a DNA polymerase inhibitor, also had no effect on nucleolar FL-SRAG-GFP (data not shown). In sum, we conclude that SRAG localization is dependent on RNA and strongly suggests that SRAG interacts with RNA.

FL-SRAG Is Down-regulated in Proliferating Cells and Can Inhibit Proliferation—In preliminary experiments, we observed that cells overexpressing SRAG grew with delayed kinetics. To explore a link between SRAG and proliferation, thymocytes were either left resting or induced to proliferate with anti-CD3 and anti-CD28 antibodies for 24 and 48 h. Total cell extracts were prepared, and Western blotting was performed for HSP90 and SRAG. When normalized to HSP90, SRAG levels decreased when thymocytes were activated (Fig. 6*A*). Because the nucleolus breaks down during mitosis at G_2/M and SRAG can occupy the nucleolus, we postulated that SRAG protein levels are reduced at the G_2/M stage of the cell cycle. To test this, HeLa cells were arrested at G_2/M with a nocodazole block. Free floating G_2/M cells were washed and replated in plain medium. Protein extracts were prepared, and a Western blot was performed for SRAG. As shown in Fig. 6*B*, SRAG was down-regulated in nocodazole-treated cells, but its expression returned after 24 h of replating in nocodazole-free medium (Fig. 6*B*). This effect is specific for G_2/M as co-treatment with aphidicolin, a DNA polymerase inhibitor that blocks cells at S phase, prevented the nocodazole-induced loss of SRAG protein (Fig. 6*C*). As a result, the loss of SRAG induced by nocodazole is the result of specific machinery active at G_2/M and not simply the drug. Consistent with that finding, other agents known to affect other stages of the cell cycle such as transforming growth factor-β, aphidicolin, thymidine, and rapamycin did not have a similar effect on SRAG protein levels (Fig. 6*D* and supplemental Fig. 2). We therefore conclude that SRAG protein levels are down-regulated by machinery at the G_2/M phase of the cell cycle.

Based upon these data, we hypothesized that the overexpression of FL-SRAG-GFP could reduce the number of cells at the G_2/M phase of the cell cycle. HeLa cells were transfected with either eGFP alone or FL-SRAG-GFP for 24 h, permeabilized, stained with propidium iodide, and analyzed by flow cytometry. After gating on eGFP$^+$ cells, the propidium iodide trace of transfected cells was determined. As shown in Fig. 6*E*, overexpression of FL-SRAG-GFP reduced the percentage of cells at G_2/M (Fig. 6*E*). In addition to decreasing the number of cells at G_2/M, it was also possible that the reduced growth observed in SRAG-transfected cells could also be attributed to an increase in cell death. To test that idea, HeLa cells were transfected with either GFP or FL-SRAG-GFP for 24 h. The cells were harvested and resuspended in PBS containing propidium iodide. Propidium iodide is cell-impermeable, and thus dead cells, which have lost membrane integrity, will stain with propidium iodide under these conditions. After gating on GFP$^+$ cells, the percentage of GFP$^+$ cells that stained with propidium iodide was determined. Although the overall level of cell death in these assays was low, SRAG did enhance cell death by 2-fold (Fig. 6*F*). As a result, the slow growth observed when SRAG was overexpressed is the combined effect of reducing entry into the G_2/M stage of the cell cycle and enhancing cell death.

DISCUSSION

The current work describes the cloning and initial characterization of SRAG, a small arginine- and glycine-rich protein that

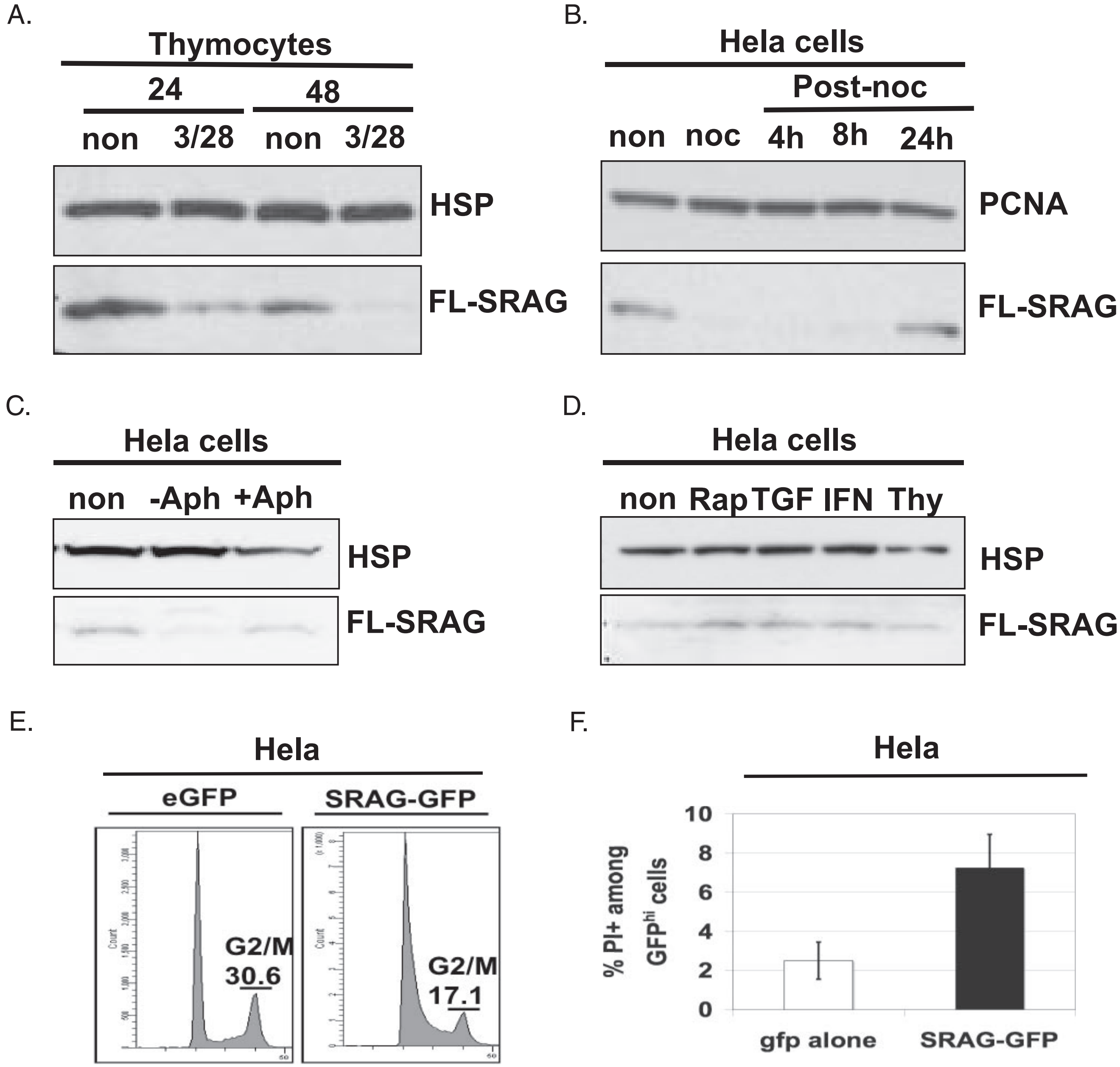

FIGURE 6. **Correlation of SRAG and proliferation.** *A*, thymocytes from wild type mice were left resting or activated with anti-CD3^{+} anti-CD28 (*3/28*) antibodies for 24 and 48 h. Total protein extracts were prepared, and a Western blot was performed for control HSP90 and SRAG. Shown are data representative of three experiments. *B*, HeLa cells were either left untreated (*non*) or treated with nocodazole (*noc*) for 16 h. Round floating G_2/M cells were harvested and replated for the time points indicated (*post-noc*). Total protein extracts were prepared, and a Western blot was performed for control proliferating cell nuclear antigen (*PCNA*) and SRAG. Shown are representative data from three experiments. *C*, HeLa cells were either left untreated (*non*) or treated with nocodazole $\pm$ the DNA polymerase inhibitor aphidicolin (*Aph*) for 16 h. Protein lysates were prepared, and a Western blot was performed for control HSP and FL-SRAG. Shown are data representative of two experiments. *D*, HeLa cells were treated with rapamycin (*Rap*; 0.5 μg/ml), transforming growth factor-β (*TGF*) (1 ng/ml), interferon α (*IFN*; 1000 units/ml), and thymidine (*Thy*; 2 mM) for 16 h. Protein lysates were prepared, and a Western blot for FL-SRAG was performed. *E*, HeLa cells were transfected with either eGFP or FL-SRAG-GFP for 24 h. Cells were harvested, permeabilized, and stained with propidium iodide. After gating on GFP^{+} cells, propidium iodide was analyzed. Shown is the percentage of G_2/M cells that is representative of three experiments. *F*, HeLa cells were transfected as in *E*. After 24 h, the cells were resuspended in PBS containing propidium iodide. After gating on GFP^{+} cells, the percentage of cells that stained with propidium iodide (dead cells) was evaluated. In all cases, the percentage of cells transfected with eGFP or FL-SRAG-GFP was similar. Shown is the average and S.D. (*error bars*) of four experiments.

is highly conserved. Aside from the arginine- and glycine-rich region, which aided in localizing SRAG to the nucleus and nucleolus, SRAG lacks known protein domains and bears little homology to other mammalian proteins. SRAG is widely expressed; however, the highest levels are found within lymphoid tissues. As the nucleolus within lymphocytes remains essentially uncharacterized, we can only speculate as to how SRAG proteins participate in lymphocyte biology.

Although extensive work has characterized the human nucleolar proteome (8–11), SRAG has not yet been detected in those studies. This most likely reflects that in HeLa cells, the model cell type for these studies, FL-SRAG-GFP is found in the nucleolus in only 25–35% of the cells. As a result, it is almost certain that more abundant nucleolar proteins mask the presence of endogenous SRAG in large scale screens. Consistent with its localization within the nucleolus, SRAG is sensitive to changes in RNA, and our data suggest that SRAG can interact with RNA molecules. Given its nucleolar localization, ribosomal RNA is a likely candidate. Our studies with actinomycin D, a well established method for disrupting ribosomal RNA and the nucleolus, support that idea. However, we cannot rule out an interaction with other RNA molecules, nor can we completely exclude an interaction with DNA.

The observation that the N terminus of SRAG acts to exclude SRAG from the nucleolus is itself novel as no other protein in available databases contains the sequence of the SRAG N terminus. In addition, although localization to the nucleus can be predicted based upon amino acid sequence, localization into the nucleolus is still somewhat difficult to predict. Although basic residues such as polyarginine are well known to drive proteins into the nucleolus (12), sequences that govern exclusion or retention are still cryptic. In the case of SRAG, we can demonstrate that the N terminus acts to exclude SRAG from the nucleolus. At this point, it is difficult to say precisely how the N terminus of SRAG regulates its localization. Thus far, we have not been able to detect an interaction between SRAG and other nucleolar proteins such as nucleolin (13) and B23 (14), which can shuttle into and out of the nucleolus. Given the ability of SRAG to impact the cell cycle, it is possible that SRAG localization within the nucleolus may be correlated with a specific cell cycle stage (15). However, analysis of SRAG localization following synchronization with both nocodazole (G_2/M) and aphidicolin (S phase) failed to yield a homogeneous population (data not shown). As a result, it is unclear how the cell manipulates the SRAG N terminus to partition SRAG between the nucleus and nucleolus.

The observation that SRAG levels are reduced at G_2/M and that SRAG overexpression can reduce the percentage of cells at G_2/M is consistent with a protein that can occupy the nucleolus. It is well known that cell division requires disassembly of the nucleolus prior to mitosis and reassembly following cytokinesis and entry into G_1 (15). The inability of SRAG-overexpressing cells to efficiently traverse to G_2/M may represent a failure in many different processes that control nuclear cell division. We believe that the increase in cell death following SRAG overexpression is an indicator of the frustrated attempt of cells to successfully traverse G_2/M. In sum, our data indicate a clear link between SRAG and the cell cycle that warrants additional study.

The ultimate test of gene function is the production of a knock-out mouse. Through the German Gene Trap Consortium, we obtained embryonic stem cells in which a retroviral gene trap has been inserted into the murine SRAG gene. Chimeras and heterozygous mutant mice were generated; however, we could not obtain homozygous mutants from heterozygote/heterozygote matings. In addition homozygous mouse embryonic fibroblasts and embryonic stem cells could not be generated. As a result, we believe that disruption of the SRAG gene is incompatible with viability. Similar results have been observed when attempting to reduce SRAG expression *in vitro* through RNA interference approaches. A conditional SRAG allele will need to be generated to study SRAG *in vivo* and confirm these preliminary observations.

In sum, our studies indicate that SRAG is a new and complex member of the nucleolar proteome. Our current work serves as the foundation on which to build our understanding of the SRAG protein. We predict that continued work with SRAG will provide multiple insights into nucleolar biology, proliferation, development, and disease.

Acknowledgments—B23-dsRed was generous gift from A. Lamond, University of Dundee, Dundee, Scotland, UK. We give special thanks to members of the Grusby and Glimcher laboratories at the Harvard School of Public Health for helpful discussions.

REFERENCES

1. Tanaka, T., Soriano, M. A., and Grusby, M. J. (2005) *Immunity* **22,** 729–736
2. Lehner, B., Semple, J. I., Brown, S. E., Counsell, D., Campbell, R. D., and Sanderson, C. M. (2004) *Genomics* **83,** 153–167
3. Olsen, J. V., Blagoev, B., Gnad, F., Macek, B., Kumar, C., Mortensen, P., and Mann, M. (2006) *Cell* **127,** 635–648
4. Wan, D., Gong, Y., Qin, W., Zhang, P., Li, J., Wei, L., Zhou, X., Li, H., Qiu, X., Zhong, F., He, L., Yu, J., Yao, G., Jiang, H., Qian, L., Yu, Y., Shu, H., Chen, X., Xu, H., Guo, M., Pan, Z., Chen, Y., Ge, C., Yang, S., and Gu, J. (2004) *Proc. Natl. Acad. Sci. U. S. A.* **101,** 15724–15729
5. Nakahira, M., Tanaka, T., Robson, B. E., Mizgerd, J. P., and Grusby, M. J. (2007) *Immunity* **26,** 163–176
6. Maison, C., Bailly, D., Peters, A. H., Quivy, J. P., Roche, D., Taddei, A., Lachner, M., Jenuwein, T., and Almouzni, G. (2002) *Nat. Genet.* **30,** 329–334
7. Hetz, C. A., Hunn, M., Rojas, P., Torres, V., Leyton, L., and Quest, A. F. (2002) *J. Cell Sci.* **115,** 4671–4683
8. Andersen, J. S., Lyon, C. E., Fox, A. H., Leung, A. K., Lam, Y. W., Steen, H., Mann, M., and Lamond, A. I. (2002) *Curr. Biol.* **12,** 1–11
9. Lam, Y. W., Lamond, A. I., Mann, M., and Andersen, J. S. (2007) *Curr. Biol.* **17,** 749–760
10. Leung, A. K., Andersen, J. S., Mann, M., and Lamond, A. I. (2003) *Biochem. J.* **376,** 553–569
11. Scherl, A., Coute, Y., Deon, C., Calle, A., Kindbeiter, K., Sanchez, J. C., Greco, A., Hochstrasser, D., and Diaz, J. J. (2002) *Mol. Biol. Cell* **13,** 4100–4109
12. Martin, R. M., Tunnemann, G., Leonhardt, H., and Cardoso, M. C. (2007) *Histochem. Cell Biol.* **127,** 243–251
13. Mongelard, F., and Bouvet, P. (2007) *Trends Cell Biol.* **17,** 80–86
14. Okuwaki, M. (2008) *J. Biochem.* **143,** 441–448
15. Boisvert, F. M., van Koningsbruggen, S., Navascues, J., and Lamond, A. I. (2007) *Nat. Rev. Mol. Cell Biol.* **8,** 574–585